Available online at www.sciencedirect.com
SCIENCE DIRECT®
Physica B 325 (2003) 46–56
PHYSICA B
www.elsevier.com/locate/physb

FP-LAPW investigations of electronic structure and bonding mechanism of NbC and NbN compounds

T. Amriou[a], B. Bouhafs[a], H. Aourag[a], B. Khelifa[b], S. Bresson[b], C. Mathieu[b,*]

[a] *Physics Department, Computational Materials Science Laboratory, University of Sidi-Bel-Abbes, 22000-Algeria, Algeria*
[b] *Faculte Jean perrin, University d'Artois, SP18-Rue Jean Souvraz, 62307 Lens cedex, France*

Received 9 October 2000; received in revised form 10 June 2002

Abstract

We have studied the structural and electronic properties of niobium nitride and niobium carbide by means of accurate first principle total energy calculations using the full-potential linearized augmented plane wave method. The calculations are based on density functional theory and we have used the local density approximation as well as the generalized gradient approximation for the exchange and correlation potential. We obtained reasonable results comparatively with the experimental data and other calculations.

Keywords: Refractory metal compounds; Transition-metal carbides; Transition-metal nitrides; Linearized augmented plane wave; First principle's calculation

1. Introduction

The transition-metal carbides and nitrides (TMCNs) possess many scientifically interesting and technologically important properties [1]. On the microscopic level they display three different types of bonding characteristics: metallic, ionic, and covalent [2–7]. This unusual combination of bonding mechanisms manifests itself in their macroscopical properties. They exhibit ultrahardness [3–5], for example, many binary carbides have microhardness values between 2000 and 3000 kg/mm^2 values which lie between those of Al_2O_3 and diamond [1]. This property has resulted in an extensive use of carbides as cutting tools and for wear-resistant surfaces. However, the nitrides are hard, but are not as hard as the carbides. A second striking property of these materials is their very high melting points as well as metallic conductivity [8]. Perhaps the important property of this type of compounds is their defect structure, they often crystallize in the sodium chloride structure [1], they are fairly simple to treat theoretically.

In this work, we choose two compounds, niobium carbide (NbC) and niobium nitride (NbN). NbC is presently one of the most important materials for hardness and corrosion resistant coating. It is used to provide solutions to the most demanding high temperature materials problems. Presently interest is also developing within the microelectronic industry for the use of NbN as an electrically conducting barrier, since it has a high superconducting critical temperature (T_c about 20 K) [9]. The success of these

*Corresponding author.
E-mail address: mathieu@univ-artois.fr (C. Mathieu).

0921-4526/02/$ - see front matter
PII: S0921-4526(02)01429-1

compound process led physicists to investigate the growth of thermally grown magnesium oxide (MgO) as a barrier in NbN junctions and to develop a trilayer process for fabrication of NbN/MgO–Mg/NbN Josephson junctions [10].

The unusual combination of properties has challenged theorists to study the chemical bonding in these compounds [5,6] because certain features of bonding that have been clarified are useful in interpreting physical properties. Some of the properties that these theories should explain, e.g., the extremely high melting points, the ability of these carbides and nitrides to form extensive solid solutions with each other and the contributions of metallic, covalent, and ionic bonding to the cohesive energy. Important bonds can be formed between both metal–metal and metal–nonmetal pairs of atoms. Most theories have attempted to determine the relative importance of each type of contribution to bonding and the relative importance of metal–metal versus metal–nonmetal bonds [11,12]. Moreover, these theories have been concerned about the direction of electron transfer between metal and nonmetal atoms. One original ideas was suggested by Hägg [10] about 60 years ago. This author tried to explain the properties of transition metal compounds involving H, C, N, and O. He started from a crystallographic point of view and studied the atomic radii of many known structures of such transition metal compounds. He observed that there is a critical value of 0.59 for the ratio between the nonmetal (X) and metal (M) radius. As long as the metalloid atom is sufficiently small (r_X/r_M is below 0.59), simple structures are found and the M–M distance are slightly larger to those in the corresponding pure metals. This observation led him to propose that these materials could be regarded as interstitial alloys rather than compounds, with the nonmetal atoms merely filling the voids in the host lattice of transition-metal atoms and that the M–M bonds are the essential bonds in comparison with the M–X bonds. But Rundle [12] gave another interpretation. He concluded from the increase of the M–M distance that a weakening of the M–M bonds occurs with some electrons forming M–X bonds which are responsible for the hardness and brittleness of these compounds. These simple ideas have been refined and improved over the years, and two distinct models have emerged. The first model stresses the importance of M–M bonds in explaining the stability and other observed properties of these material. The second model attributes these properties to the formation of M–X bonds.

In order to test the validity of these models, there has been some investigations using pseudopotential [13], APW [14], and tight binding methods [4–7]. In this paper we present the results of studies of the electronic structures of stoichiometric NbC and NbN. The calculations have been done using the full-potential linearized augmented plane wave (FP-LAPW) method [15–19] based on the density functional theory.

2. Details of calculations

In our calculations, the electronic structure of the NbC and NbN is calculated within the density functional theory (DFT) [20–22] formalism using the local-density approximation (LDA), parametrized by Hedin and Lundqvist [23,24], as well as a gradient corrected functional (GGA-PBE), parametrized by Perdew et al. [25,26], for the exchange and correlation potential. Total energies and all derived quantities are obtained using first principles full potential linearized augmented plane wave (FP-LAPW) method [17–19]. Extended test calculation have proven to yield sufficient accuracy in total energy minimization of bulk NbC and NbN using only 20k points inside the irreducible part of the Brillouin zone, an energy cut-off of the plane wave expansions in the interstitial region of $RK_{max} = 8$, and $l_{max} = 10$ for the upper limit of the angular momentum expansions of the wave functions inside the nonoverlapping spheres surrounding the atomic sites. The radial basis functions within the muffin-tin spheres are linear combinations of radial wave functions and their energy derivatives, computed at energies appropriate to their site. Outside the muffin-tin spheres the basis functions are plane waves expanded in a Fourier series. All results represented here are obtained with a convergence of the order of 1 mRy in the energy eigenvalues. The ab initio calculation of the valence and conduction band energy

eigenvalues has been performed at 111 points including five high symmetry points W, L, Γ, X, and K.

In this work, the states treated as bands were: Nb(4s, 4p, 4d, 5s), N(2s, 2p) and C(2s, 2p), the muffin-tin radii chosen are 2.1, 1.8, and 1.9 a.u. for Nb, N, and C, respectively. Self-consistently of the band eigenvalues was achieved after seven iterations. We also mentioned that the type of radial equation used in this work is semirelativistic as derived by Harmon and Koelling [29]. Moreover, comparative studies on bulk NbC and NbN with the LDA and the GGA show small differences that do not affect the present conclusions. Therefore, in the following only results from calculation within the LDA scheme will be discussed.

3. Results and discussions

3.1. Structural and elastic properties

In Fig. 1 we show the total energy curve as a function of unit cell volume for NbC and NbN. For the determination of static equilibrium properties, we use the Murnaghan equation of states [30].

In Table 1, we give our calculated values of the equilibrium lattice constants, bulk modulus, and its pressure derivative for NbC and NbN, as well as the experimental and other theoretical values. We notice from these tables that our LDA results for the equilibrium lattice constants are slightly smaller about 0.9% and 0.6% than the experimental values for NbC and NbN, respectively. However, when we use the GGA these calculated lattice constants are slightly larger about 0.5–0.9% of the experimental values for NbC and NbN, respectively. For the calculated values of the bulk modulus (B), we have noticed that the value given by the LDA for NbC is overestimated with regards to the experimental value by 7%, whereas the GGA result underestimated it by 3%. For NbN, the calculated value of B in the LDA is larger than the experimental value about 9.5%, while the GGA value is underestimated by 4%.

To calculate the elastic constants, we have used the procedure of Mehl [31]. Our calculated elastic

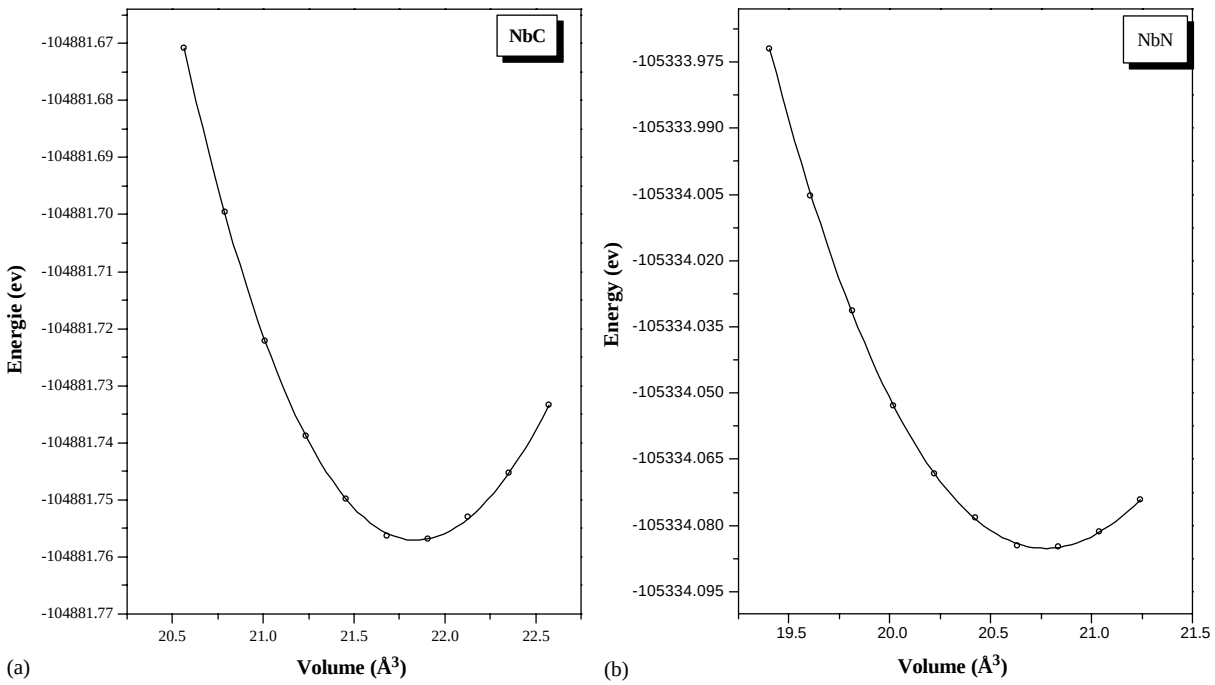

Fig. 1. Total energy as a function of lattice constant obtained by LDA calculations of (a) NbC and (b) NbN.

Table 1
Calculated and experimental lattice constant a_0, bulk modulus B, their energy derivative B', and elastic constants of NbC and NbN

	NbC					NbN		
	LDA	GGA	Exp.	LAPW	TB	LDA	GGA	Exp.
a_0(Å)	4.43	4.49	4.470[a]	—	—	4.363	4.430	4.390[a]
B(Mbar)	3.28	2.93	3.02[a]	3.32[e]	—	3.499	3.074	3.20[a]
B'	4.88	4.56	—	—	—	4.922	4.214	—
C_{11}(Mbar)	6.27	5.46	6.2[d]	6.4[e]	8.62[f]	6.04	4.98	5.56[b]
C_{12}(Mbar)	1.79	1.67	2.00[c]	1.8[e]	1.60[f]	2.23	2.12	1.52[b]
C_{44}(Mbar)	2.20	2.24	1.50[c]	1.4[e]	0.51[f]	1.84	0.89	1.25[b]

[a] Ref. [1].
[b] Ref. [37].
[c] Ref. [36].
[d] Ref. [38].
[e] Ref. [32].
[f] Ref. [39].

constants are listed in Table 1. For NbC we see that the calculated values of C_{11} and C_{44} in the LDA are larger than the experimental values, but C_{12} is underestimated. When we use GGA, these calculated values of C_{11} and C_{12} are underestimated, and C_{44} overestimated in comparison with the experimental data. For NbN, within LDA, our calculated values of C_{11}, C_{12} and C_{44} are underestimated than the experimental values, but GGA reduced the values of C_{11} and C_{44}, and C_{12} remains higher than the experimental values.

3.2. Electronic structure results

3.2.1. Band structure

In Fig. 2, we show our LDA calculations of the band structures in the rock-salt structure of NbC and NbN compounds. The band order using the GGA is very similar to that found by LDA, thus we show only the LDA band structure. The band structures and band ordering for NbC and NbN are seen to be very similar in the region below the Fermi energy. They are characterized by an energetically low-lying band, which is derived from the 2s states of the nonmetal atoms and which do not contribute to the bonding. These bands display a maximum dispersion between Γ and L of values 0.282 and 0.198 Ry for NbC, and NbN, respectively. This difference is due to the energy separation between the 2s-X and 2p-X bands. The next lowest bands originate mainly from 2p-X in some part of the Brillouin zone and 4d-Nb in another part of the zone, as can be seen by an overlap and a mixing between these bands when we are going from Γ to X(Δ). These results is in qualitative agreement with X-ray emission spectra found by Ramqvist et al. [33], and Källne and Pessa [34]. The niobium d-bands are further decomposed into t_{2g}, which originates from $\Gamma_{25'}$ at the centre of the BZ and the e_g bands originating from Γ_{12}. The highest band shown in these figures originate from 5s-Nb, because in these compounds, the repulsive interaction with the nonmetal 2s-band shifts this band to higher energies above the Fermi level in both NbC and NbN. These higher metal 5s states do not mix strongly with the metal d-band, but rather lie (0.56 and 0.27 Ry) above the Γ_{12} level for NbC and NbN, respectively.

In Tables 2 and 3, the values of characteristic band separations are given. We have selected for comparison the gap E_g between the X s-band and the second valence-band complex at L points, the zone-center d-band splitting $\Delta E_d \equiv E(\Gamma_{12}) - E(\Gamma_{25'})$, the metal-d nonmetal-p splitting $E_d - E_p = [\frac{2}{5}E(\Gamma_{12}) + \frac{3}{5}E(\Gamma_{25'})] - E(\Gamma_{15})$ (*which is one measure of the relative positions of the* Nb d *and* X p-*bands*), and the X-p X-s splitting $E_p - E_s = E(\Gamma_{15}) - E(\Gamma_1)$ (*also defined the relative positions of* X p *and* X s-*bands*). We have also selected other energy difference given by

$E(\Gamma_{15}) - E(L_1)$: width of the 2p-bands.

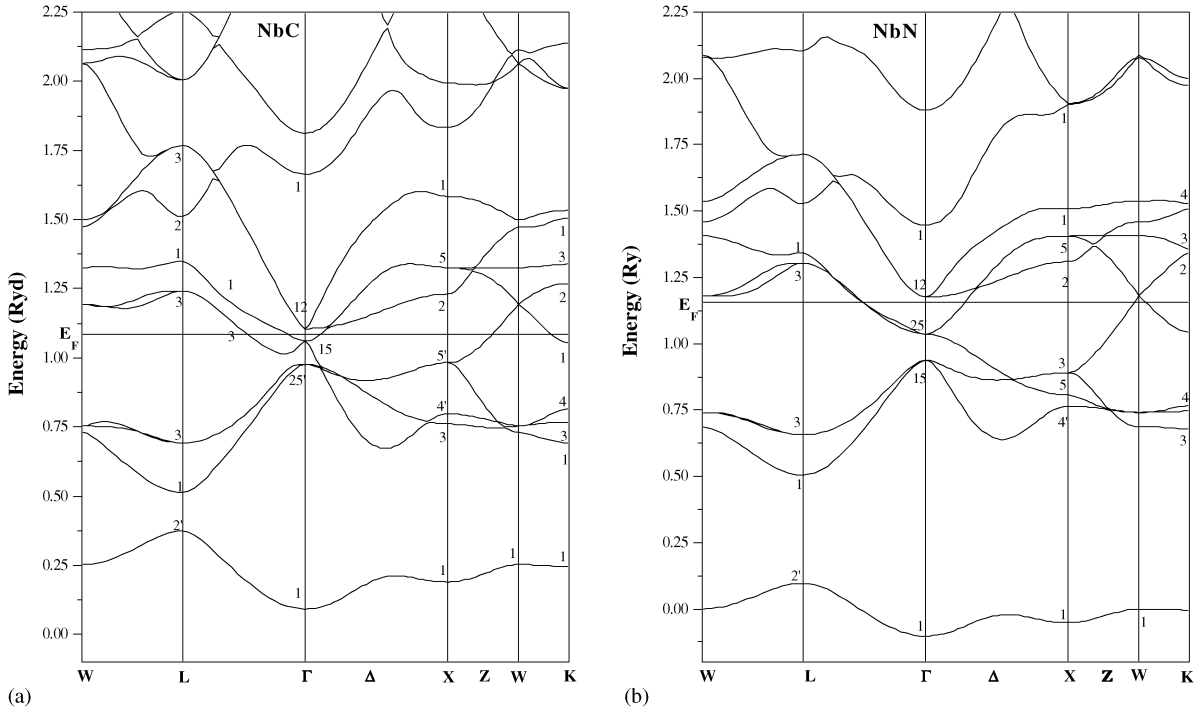

Fig. 2. Electronic energy band structure obtained by the LDA calculation of (a) NbC and (b) NbN.

Table 2
Comparison of important energy gaps obtained from LAPW and APW calculations for NbC. The entries are in Ry

	LDA[a]	GGA[a]	APW[b]
E_F	1.08494	1.05548	0.770
E_g	0.13815	0.17322	0.250
ΔE_d	0.12817	0.11890	0.133
E_d-E_p	−0.0321	−0.0306	0.150
E_p-E_s	0.96881	0.96515	0.870
$\Gamma_{15} - L_1$	0.54791	0.53120	0.429
$E_F - L_1$	0.57217	0.55396	0.579
$E_F - X_3$	0.39200	0.30644	0.270

[a] Reference. Our results.
[b] Ref. [7].

$E_F - E(L_1)$: width of the occupied part of the 2p and 4d-bands in the case of overlap.

$E_F - E(X_3)$: width of the occupied part of the 4d-bands.

The essential features of the band structure found in our calculations are in a good agreement with the results reported by Klein [6] using LCAO method, Mattheiss and Gupta [7] using the APW method, and many others [27–40]. In comparison, we notice that the Fermi level moves up in energy, since the number of valence electrons increase from eight to nine for NbC and NbN, respectively. Therefore, the increase in E_F is caused by the additional valence electron. From Tables 2 and 3, one can clearly see that the width of the nonmetal p band from L_1 to Γ_{15} is larger for NbC than for NbN, because in these bands, there is a strong hybridization of pd_σ and pd_π in NbC. It is interesting to note that the E_g values at X-points (in order of ≈ 0.714 Ry) for NbN is greater than in NbC (with $E_{gx} = 0.584$ Ry), indicative of the increase of the ionicity in NbN in comparison with NbC. However, the quantity $E_d - E_p$, which is a measure of the relative positions of the Nb-4d and X-2p bands, increases from NbC to NbN, indicative of the decrease of the overlap and mixing between these two bands. So we can deduce that there is a decrease of covalency in these

Table 3
Comparison of important energy gaps obtained from LAPW, EPM, APW, and SC-APW calculations for NbN. The entries are in Ry

	LDA[a]	GGA[a]	APW[b]	APW-SC[c]	APW[d]	EPM[e]
E_F	1.15571	1.14618	—	—	—	—
E_g	0.40748	0.45550	0.44000	—	—	—
ΔE_d	0.13989	0.13264	0.15000	0.14470	0.13523	0.14699
E_d-E_p	0.15366	0.15147	0.16000	0.14170	0.43920	0.14258
E_p-E_s	1.05024	1.04230	1.05000	0.48060	0.71070	0.47920
$\Gamma_{15} - L_1$	0.43381	0.41659	—	0.41673	0.26312	0.35573
$E_F - L_1$	0.68128	0.65475	—	—	—	0.59827
$E_F - X_3$	0.29483	0.28804	—	—	—	—

[a] Reference. Our results.
[b] Ref. [40].
[c] Ref. [35].
[d] Ref. [42].
[e] Ref. [43].

compounds. Therefore, the covalent component is strongest in the carbide and reduced in the nitride. These covalent interactions in these compounds occur mainly between X 2p and Nb 4d atomic states. It is interesting to note that $E_d - E_F$ for NbC, about -0.04 Ry, is an indication also of the strong hybridization between metal and nonmetal states near E_F.

We have mentioned above that $E_F - L_1$ denotes the width of the occupied part of the 2p and 4d-bands, this last quantity increases from NbC to NbN. Therefore, we suggest that they give an adequate description because the extra electron added in NbN goes primarily into filling d-states.

There are some crucial differences like a significant difference in the band ordering at the Γ point for NbC in comparison with NbN. If we examine, for example, the band structure of NbC, given by Gupta and Freeman [6], and those given by Chadi and Cohen [35], we can see that Γ_{15} lies below $\Gamma_{25'}$ levels just below E_F. But Schwarz [33] obtained the opposite ordering. In order to distinguish between these two pictures, we give in Tables 4 and 5 further informations relevant to our band structure at Γ points for NbC and NbN.

From these tables we found that, our band ordering is very similar to those given by Schwarz [33]. The differences that exist can be attributed to the self-consistency, which we include and he does not. In this situation, where we have a significant charge transfer and band hybridization, the self-consistent effect is very important for a reliable band-structure picture.

3.2.2. Bonding mechanism

Referring always to Fig. 2, we can clearly assume that there is a mixing and overlap between nonmetal p and niobium d-bands in the Γ to X(Δ) direction in the Brillouin zone. For this reason, we have selected one k-point, namely $\Delta = \pi/a(1,0,0)$ halfway between Γ and X, and we have noted all possible cases for the hybridization (*we have omitted the antibonding states*).

In combining the different results of Tables 6 and 7, we can deduced that in the p-band the nonmetal p-like charge always dominates in all compounds. However, we have noticed that in the NbC both partial charges e_g and t_{2g} have large values indicating the presence of strong pd_σ and pd_π in the Δ_1 and Δ_5 bands, respectively. In NbN these Nb-d partial charges are much smaller, therefore the p–d interaction is reduced. In the d-band of NbN unlike NbC, the Nb-d(t_{2g}) charge exceeds all other components and leads to a strong dd_σ bond. From these results, it is reasonable to note that the stability and other observed properties of these materials can be explained by the formation of M–X bonds studied by Rundle [12] without excluding the relative importance of other effects such as the d–d interaction especially for NbN compound [11].

Table 4
LAPW partial charge in the Γ points for NbC

		Γ_1	Γ_{15}	$\Gamma_{25'}$	Γ_{12}
Energy (Ry)		0.09186	1.06068	0.97729	1.10545
	s	8.889	—	—	—
Nb-sphere	p	—	1.803	—	—
	$d(e_g)$	—	—	—	68.826
	$d(t_{2g})$	—	—	58.353	—
	s	51.403	—	—	—
C-sphere	p	—	73.861	—	—
	$d(e_g)$	—	—	—	6.769
	$d(t_{2g})$	—	—	3.647	—

Table 5
LAPW partial charge in the Γ points for NbN

		Γ_1	Γ_{15}	$\Gamma_{25'}$	Γ_{12}
Energy (Ry)		−0.101100	0.93823	1.03596	1.175820
	s	6.583	—	—	—
Nb-sphere	p	—	1.623	—	—
	$d(e_g)$	—	—	—	69.896
	$d(t_{2g})$	—	—	59.235	—
	s	63.812	—	—	—
N-sphere	p	—	76.560	—	—
	$d(e_g)$	—	—	—	5.635
	$d(t_{2g})$	—	—	2.992	—

Table 6
LAPW partial charge along the Δ direction for NbC

		Δ_1	Δ_1	Δ_5	$\Delta_{2'}$
Energy (Ry)		0.199200	0.67900	0.92050	0.85020
	s	4.894	2.158	—	—
Nb-sphere	p	3.212	1.255	3.187	—
	$d(e_g)$	2.940	20.561	—	—
	$d(t_{2g})$	—	—	20.955	48.642
	s	56.168	1.150	—	—
C-sphere	p	0.120	40.079	42.913	—
	$d(e_g)$	0.108	0.095	—	—
	$d(t_{2g})$	—	—	0.442	3.891
	Bonding		pd_σ	pd_π	dd_σ

Table 7
LAPW partial charge along the Δ direction for NbN

		Δ_1	Δ_1	Δ_5	$\Delta_{2'}$
Energy (ev)		−0.02299	0.64230	0.86290	0.90070
	s	3.096	2.541	—	—
Nb-sphere	p	3.320	1.449	3.275	—
	$d(e_g)$	2.044	14.813	—	—
	$d(t_{2g})$	—	—	9.731	48.915
	s	68.272	0.473	—	—
N-sphere	p	0.015	47.473	59.547	59.547
	$d(e_g)$	0.052	0.035	—	—
	$d(t_{2g})$	—	—	0.153	3.141
	Bonding		pd_σ	pd_π	dd_σ

3.2.3. *The density of states*

In Fig. 3, we show only the total and partial density of states (DOS) for NbX (with X denote C and N) as obtained by means of the LDA, since they are very similar to those obtained by the GGA with only a slight differences in the energy levels. The DOS of the valence and conduction bands are characterized by two regions separated by a gap, the lower region is of X-s character of the nonmetal atoms, with a very small contribution of the Nb-d component with e_g manifold of metal atoms. This band is lowered going from NbC to NbN, following the increasing electronegativity. It is very interesting to note the overall similarity among all these curves in the second region, characterized by two high-density peaks separated by a low-density region. In this second region, exactly in the first peak, we can see that the nonmetal-p density of states dominates on the two compounds, but the mixture of the $d(t_{2g})$ and $d(e_g)$ manifolds in this range of energy is considerably higher in NbC than in NbN. An important points to note is that the partial DOS are useful for interpreting the bonding mechanism. In NbC and NbN, we have two types of bonds in the region where p-bands dominate. The first one is due to the $d(e_g)$ symmetry which can form a pd_σ bond with p-orbitals of nonmetal atoms. Similarly, $d(t_{2g})$ orbitals are involved in pd_π bonds (see Table 5). We have mentioned above that the e_g and t_{2g} manifolds are smaller in NbN than in NbC, therefore we can deduced that this is weaker in NbN compared to NbC. In the range between 0.85 Ry and E_F, the niobium d-component of the DOS dominates, and it can be seen that in this energy range the t_{2g} manifold exceeds all other components. This t_{2g} charge can form dd_σ bonds between neighboring niobium atoms because the

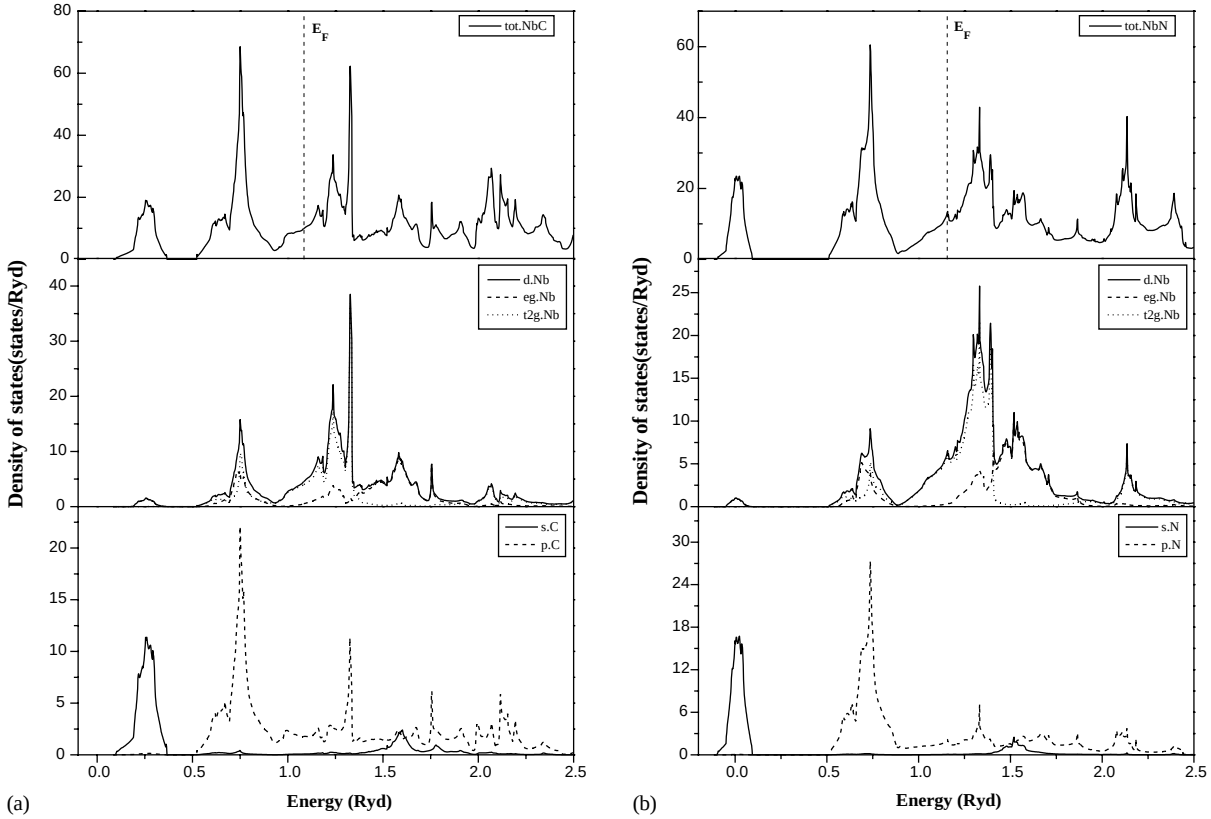

Fig. 3. The density of states (DOS) obtained by the LDA calculation of (a) NbC and (b) NbN (in states per Ry unit cell).

nonmetal p contributions to the DOS are small, so not the pd_{π} but the dd_{σ} bonds are most important.

From Fig. 3, we have observed that there is always a shape minimum in the density of states. When the band is filled with eight valence electrons, as in the case of NbC, this minimum of the density of state separated the bonding from the antibonding bands. But in the case of NbN, this shape minimum is further from the two states mentioned above, because in this compound the occupied DOS close to the Fermi level contains more d-electrons than in NbC. Therefore, the additional valence electrons cause the Fermi energy to rise above this minimum. We also suggest that the limited overlap between 2p-X and 4d-Nb states is responsible for the sharp decrease in the value of the density of states at this minimum.

From Fig. 3, we can deduce the values of the DOS at Fermi energy, obtained by the FP-LAPW method for NbC which is 9.8527 states/Ry unit cell, in good agreement with the experimental values reported by Toth [1] from electronic specific-heat measurement (9.79 states/Ry unit cell). Furthermore, our value is much better than that obtained by Schwarz [4] using the APW method (8.5 states/Ry unit cell), and that given by Klein et al. [6] using the LCAO-CPA method (8.331 states/Ry unit cell). In the case of NbN, our obtained value is about 11.025 states/Ry unit cell, which is close to the experimental value found by Toth 11.4288 states/Ry unit cell, and it is better than those obtained by Schawrz [36] (13.333 states/Ry) and by Gupta [7] (8.67 states/Ry unit cell) using the APW method.

From these values, the density of states at the Fermi level for NbN is larger than that for NbC,

which may be attributed to the higher superconducting transition temperature found in NbN. Furthermore, if we compare these densities with those obtained for the transition metal niobium (12.381 states/Ry unit cell) [1], we suggest that the niobium nitride is a good metallic conductor with conductivity comparable to that of the parent transition metal.

3.2.4. Valence electron density

From Fig. 4, there seems to be no doubt that the charge transfer is from the metal to the nonmetal sphere. From Table 8, we have the difference in the electronic charge inside the atomic sphere between the crystal (LAPW) value $Q_{\text{crystal}}^{\text{sphere}}$ and the superposed atomic value $Q_{\text{super}}^{\text{sphere}}$, which is the quantity we define for studying charge transfer in a

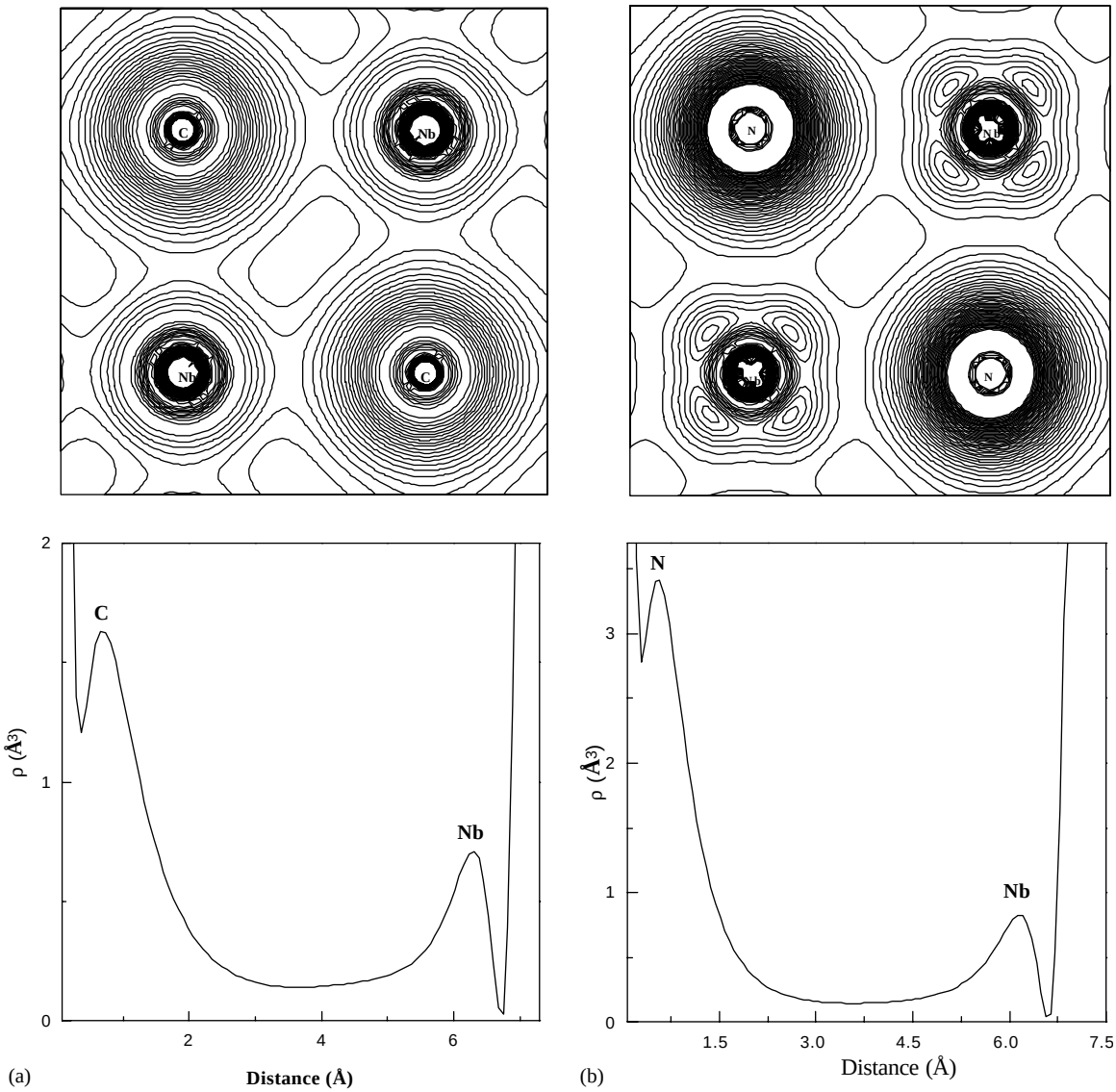

Fig. 4. Contour plot of the valence charge density in the (100) plane obtained by the LDA calculation of (a) NbC and (b) NbN.

Table 8
LAPW partial charges of different valence bands for NbC and NbN. All entries are in number of electrons per unit cell

	NbC		NbN	
Inside atomic spheres	Nb	C	Nb	N
LAPW core	28	2	28	2
Valence s	2.057	1.264	2.049	1.481
p	5.805	2.355	5.786	3.142
d	1.874	0.069	1.917	0.066
Higher	0.034	0.011	0.050	0.009
Total $Q^{in}_{crystal}$	37.770	5.699	37.802	6.698
Atomic superposed Q^{in}_{atomic}	38.294	5.307	38.275	6.263
$Q^{in}_{crystal} - Q^{in}_{atomic}$	−0.524	0.392	−0.473	0.435
Outside atomic spheres				
Total $Q^{out}_{crystal}$	3.531		3.550	
Atomic superposed Q^{out}_{atomic}	3.399		3.462	
$Q^{out}_{crystal} - Q^{out}_{atomic}$	0.132		0.038	

compound. From this table we can observe that for both NbC and NbN there is a charge transfer of about half an electron from the metal to the nonmetal atoms. Our results are similar to those given by other self-consistent band structure calculations [7,19] and are in good agreement with the electron-spectroscopy for chemical analysis (ESCA) measurement done by Rumquist [41], which shows an excess of half an electron associated with the X-sites.

Our calculations show that the valence electron density of NbN compound is not spherically symmetric around the niobium although the muffin-tin approximation is used for the potential, while the valence electrons density is always spherically symmetric around the nonmetal atoms. In niobium carbide, the valence densities around C and Nb are spherically symmetric. This point is further emphasized by calculating the ratio $(N^{Nb}_{d-t_{2g}}/N^{Nb}_{d-e_g})$ with the values 1.30 and 2.14 for NbC and NbN, respectively. We know that a symmetric density would be obtained only if orbitals with t_{2g} and e_g symmetry are occupied in the ratio of $\frac{3}{2}$ according to their degeneracies. However, we see that for NbN, t_{2g} charge depletion has considerably increased this ratio, because the extra electron in NbN goes into filling $d(t_{2g})$ states. Therefore, we note that any non spherical environment will lead to deviation from the $\frac{3}{2}$ ratio.

4. Conclusion

In the present papers new results on the electronic structure of NbC and NbN are presented and compared with experimental data and other results obtained by different methods. The good agreement between the experimental and theoretical density of state at Fermi energy, and the quantity of the charge transferred, confirms that the present LAPW results for all compounds present a fairly accurate picture of the occupied part of the band structure. At this points it is useful to discuss the general remarks that can be made for these refractory metal carbides and nitrides. We have shown that charge transfer from metal to nonmetal atoms has a great influence on the bonding in these materials, and their stability is determined by the formation of strong metal–nonmetal bonds (p–d). We do not exclude the relative importance of other effects such as the d–d interaction (metal–metal bonds), specially, for NbN.

Acknowledgements

The authors would like to thank Pr P. Blaha and all the Wien group members for providing us with their LAPW package.

References

[1] L.E. Toth, Transition Metal Carbides and Nitrides, Academic, New York, 1971;
E.K. Storms, The Refractory Carbides, Academic, New York, 1967.
[2] A. Fernandez Guillermet, J. Häglund, G. Grimvall, Phys. Rev. B 45 (1992) 11 557.
[3] K. Schwarz, J. Phys. C 10 (1977) 195.
[4] K. Schwarz, Solid State Mater. Sci. 13 (3) (1987) 211.
[5] P. Blaha, K. Schwarz, Int. J. Quantum Chem. XXIII (1983) 1535.
[6] B.M. Klein, D.A. Papaconstantopoulos, L.L. Boyer, Phys. Rev. B 22 (1980) 1946.
[7] M. Gupta, A.J. Freeman, Phys. Rev. B 14 (1976) 5205.
[8] P.A.P. Lindberg, L.I. Johansson, J.B. Lindström, P.E.S. Persson, Phys. Rev. B 12 (1987) 6343.
[9] T.H. Geballe, B.T. Matthias, J.P. Remeika, A.M. Glogston, V.B. Compton, J.P. Maita, H.J. Williams, Physics 2 (1966) 293.

[10] G.L. Kerber, An improved NbN integrated circuit process featuring thick NbN ground plane and lower parasitic circuit inductances, IEEE Trans. Appl. Supercond. 7 (1997) 2638–2643.
[11] G. Hägg, Gesetzmässigkeiten im Kristallban bei Hybriden, boriden, carbiden und nitriden der Übergangselemente, Z. Phys. Chem. B 12 (1931) 33.
[12] R.E. Rundle, A new interpretation of intertitial compounds-metallic carbides, nitrides and oxides of composition MX, Acata Crystallogr. 1 (1948) 180.
[13] K. Schwarz, Phys. Rev. B 5 (1972) 2466.
[14] D.J. Chadi, M.C. Cohen, Phys. Rev. B 10 (1974) 496.
[15] O.K. Andersen, Solid State Commun. 13 (1973) 133; O.K. Andersen, Phys. Rev. B 12 (1975) 3060.
[16] D.D. Foelling, J. Phys. Chem. Solids 33 (1972) 1335.
[17] D.J. Singh, Plane Waves, Pseudopotentials and the LAPW Method, Kluwer Academic Publishers, Boston, Dordrecht, London, 1994.
[18] E. Wimmer, H. Krakauer, M. Weinert, A.J. Freeman, Phys. Rev. B 24 (1981) 864; M. Weinert, E. Wimmer, A.J. Freeman, Phys. Rev. B 26 (1982) 4571.
[19] P. Blaha, K. Schwarz, P. Sorantin, Comput. Phys. Commun. 59 (1990) 399.
[20] N.H. March, S. Lundqvist (Eds.), Theory of the Inhomogeneous Electron Gas, Plenum, New York, 1983.
[21] W. Kohn, L.J. Sham, Phys. Rev. A 140 (1965) 1133.
[22] R.M. Dreizler, E.K.U. Gross, Density Functional Theory, Springer, Berlin, 1990; R.G. Parr, W. Yang, Density of Atoms and Molecules, Oxford University Press, Oxford, 1989.
[23] G. Ortiz, Phys. Rev. B 45 (1992) 11 328.
[24] C. Bowen, G. Sugiyama, B.J. Alder, Phys. Rev. B 50 (1994) 14 838; S. Soroni, D.M. Ceperley, G. Senatore, Phys. Rev. Lett. 75 (1995) 689.
[25] J.P. Perdew, K. Burke, M. Ernzerhof, Phys. Rev. Lett. 77 (1996) 3865.
[26] C.J. Umrigar, X. Gouze, in: D.A. Browne, et al., (Eds.), High Performance Computing and its Application to the Physical Sciences, Proceeding of the Mardi Gras 1993 Conference, World Scientific, Singapore, 1993.
[27] G. Lehmann, M. Tant, On the numerical calculation of the density of states and related properties, Phys. Stat. Sol. B 54 (1972) 469.
[28] J.D. Pack, H.J. Monkhorst, Phys. Rev. 16 (1977) 1748.
[29] D.D. Koelling, B.N. Harmon, J. Phys. C 10 (1977) 3107.
[30] F.D. Murnaghan, Proc. Natl. Acad. Sci. USA 30 (1944) 244.
[31] M.J. Mehl, Phys. Rev. B 47 (1993) 2493.
[32] J. Chen, L.L. Boyer, H. Krakauer, M.J. Mehl, Phys. Rev. B 37 (1988) 3295.
[33] L. Ramqvist, B. Ekstig, E. Noreland, R. Manne, J. Chem. Phys. Solids 32 (1971) 149.
[34] E. Källne, M. Pessa, J. Phys. C 8 (1975) 1986.
[35] K. Schwarz, Monatsh. Chem. 102 (1972) 1400.
[36] K. Schwarz (private communication) in W. Weber, Phys. Rev. B 8 (1973) 5082.
[37] J.O. Kim, J.D. AcheNbach, P.B. Mirkarimi, M. Shinn, S.A. Barnett, J. Appl. Phys. 72 (1992) 1805.
[38] H.G. Smith, Gläser, Phys. Rev. Lett. 25 (1970) 1611.
[39] M.J. Mehl, D.A. Papaconstantopoulos, Phys. Rev. B 54 (1996) 4519.
[40] D.A. Papaconstantopoulos, Phys. Rev. B 31 (1985) 752.
[41] L. Ramqvist, J. Appl. Phys. 42 (1971) 2113.
[42] L.F. Matthias, Phys. Rev. B 5 (1972) 315.
[43] C.Y. Fong, M.L. Cohen, Phys. Rev. B 6 (1972) 3635.